

---

**Keigo Nakamura<sup>1</sup>**

Naoka Nagamura<sup>2</sup>, Keiji Ueno<sup>3</sup>, Takashi Taniguchi<sup>2</sup>, Kenji Watanabe<sup>2</sup>  
and Kosuke Nagashio<sup>1</sup>

<sup>1</sup>The University of Tokyo, 7-3-1 Hongo, Bunkyo-ku, Tokyo 113-8656, Japan

<sup>2</sup>National Institute of Materials Science, 1-1 Namiki, Tukuba, Ibaraki 305-0044, Japan

<sup>3</sup>Saitam University, 255 Shimo Okubo, Sakura-ku, Saitama 338-8570, Japan

nakamura@ncd.t.u-tokyo.ac.jp

---

## Selection Mechanism of Band Alignment in 2D $p^+/n$ Tunnel FET

Tunnel field effect transistors (TFETs) are promising for the low power switching FETs which can overcome the theoretical limitation of the subthreshold swing ( $S.S. = 60 \text{ meV/dec}$ ) for conventional MOSFETs [1]. 2D-materials are expected to be suitable for TFETs because 2D-TFETs have short tunnel distance defined by van der Waals heterointerface, thereby gaining higher on-current than that for conventional 3D-TFETs. Although the  $p^+/n$  heterostructure is necessary to achieve the low  $S.S.$ , doping technique is still under development for both interstitially and chemically. Recently, we have found that  $p^+$ -WSe<sub>2</sub> doped chemically by WO<sub>x</sub> can be stabilized in air by transferring it on  $h$ -BN, and observed band-to-band tunneling (BTBT) current in the  $p^+$ -WSe<sub>2</sub>/4-layer (L) MoS<sub>2</sub> heterostructure [2]. However, its band alignment could not be changed from type II to type III even by applying the sufficient gate bias, although type-III band alignment is necessary to gain large BTBT current. In this study,  $p^+$ -WSe<sub>2</sub>/MoS<sub>2</sub> heterostructures consisting of 1 - 5L MoS<sub>2</sub> were fabricated and their transport properties were investigated in order to reveal the MoS<sub>2</sub> thickness dependence on the band alignment of charge-transfer-type  $p^+/n$  heterostructure and achieve type-III band alignment.

$p^+$ -WSe<sub>2</sub> needs to be stable in air for the source of TFET. After forming WSe<sub>2</sub>/WO<sub>x</sub> by O<sub>3</sub> annealing at 200 °C for 1 h, WO<sub>x</sub> side is transferred onto  $h$ -BN and  $p^+$ -WSe<sub>2</sub> is stabilized. After that, MoS<sub>2</sub> with suitable thickness (1 - 5L) is chosen by its contrast on PDMS and the  $p^+$ -WSe<sub>2</sub>/MoS<sub>2</sub> heterostructures were fabricated via dry transfer method using PDMS under the alignment system. Ni/Au was deposited as source/drain electrodes after the electrode pattern formation by an electron beam lithography. Then, Y<sub>2</sub>O<sub>3</sub> buffer layer (~1.5 nm), ALD-Al<sub>2</sub>O<sub>3</sub> oxide layer (~30 nm) and Al top-gate electrode were formed. **Figure 1** shows (a) schematic illustration and (b) optical image of the top-gate  $p^+$ -WSe<sub>2</sub>/2L-MoS<sub>2</sub> TFET device.

Firstly, the  $p^+$ -WSe<sub>2</sub>/3L-MoS<sub>2</sub> device with 30-nm-Al<sub>2</sub>O<sub>3</sub> was fabricated. This device consists of thinner MoS<sub>2</sub> and Al<sub>2</sub>O<sub>3</sub> than those in the previous  $p^+$ -WSe<sub>2</sub>/4L-MoS<sub>2</sub> device with 60-nm-Al<sub>2</sub>O<sub>3</sub> showing the type-II band alignment [2]. **Figure 2** shows the diode properties of 3L-MoS<sub>2</sub> device with various top gate voltage ( $V_{TG}$ ) at 20 K. The current at reverse bias is due to BTBT because minority carriers have been suppressed at sufficiently low temperature. When  $V_{TG}$  is -9 ~ 15 V, BTBT current can flow at reverse bias and negative differential resistance (NDR) trend is clearly observed as the intersection of BTBT current and diffusion current at forward bias. The appearance of NDR trend indicates that type-III band alignment is achieved.

**Figure 3(a)** compares  $I_{DS}$ - $V_{TG}$  at  $V_{SD} = -2 \text{ V}$  (reverse bias) between the 3L-MoS<sub>2</sub> and previous 4L-MoS<sub>2</sub> devices. Higher on-current can be obtained in the 3L-MoS<sub>2</sub> device than that in the 4L-MoS<sub>2</sub> device mainly owing to type-III band alignment.  $S.S.$  of the 3L-MoS<sub>2</sub> device does not depend on the temperature and is increased by increasing  $I_{DS}$ , as shown **Fig. 3(b)**. These characteristics also support that the current at reverse bias is indeed due to BTBT and  $p^+$ -WSe<sub>2</sub>/3L-MoS<sub>2</sub> device is operated as TFET.

In order to reveal the relationship between MoS<sub>2</sub> thickness and the band alignment in  $p^+$ -WSe<sub>2</sub>/MoS<sub>2</sub> device, **Figure 4(a)** compares diode properties of  $p^+$ -WSe<sub>2</sub>/1-5L MoS<sub>2</sub> devices at  $V_{TG} = 15 \text{ V}$  and 20 K. The 3L-MoS<sub>2</sub> device is only the type-III, while the other devices are the type-II because 1, 2 and 4L MoS<sub>2</sub> devices show BTBT current only at large reverse bias and the 5L-MoS<sub>2</sub> device does not show BTBT current even for reverse bias of -2 V. The brown arrows in **Fig. 4(a)** are defined as BTBT onset voltage ( $V_{BTBT}$ ), which implies band offset between the conduction band minimum (CBM) for MoS<sub>2</sub> and the valance band maximum (VBM) for  $p^+$ -WSe<sub>2</sub>. So  $V_{BTBT}$  can be modulated by  $V_{TG}$  and ideally reaches 0 V when band alignment is changed from type II to type

III for the 3L-MoS<sub>2</sub> device, as shown in Fig. 4(b). However,  $V_{\text{BTBT}}$  saturates before reaching 0 V for the other devices, although it is evident that Fermi level ( $E_F$ ) in MoS<sub>2</sub> is sufficiently modulated for all the thickness cases. This suggests that the restriction to type II results from  $p^+$ -WSe<sub>2</sub>, not from MoS<sub>2</sub>, that is,  $E_F$  in WSe<sub>2</sub> is apart from VBM due to the  $p$ -doping reduction. For this  $p$ -doping reduction in WSe<sub>2</sub>, two different origins can be considered. One is electron transfer from MoS<sub>2</sub>; the other is that the top gate modulates  $p^+$ -WSe<sub>2</sub> as well as MoS<sub>2</sub>.

Figure 5 illustrates band alignments controlled by above-mentioned two different physical origins. When  $p^+$ -WSe<sub>2</sub> is contacted with MoS<sub>2</sub>, electron is transferred from MoS<sub>2</sub> to WSe<sub>2</sub> and  $E_F$  of WSe<sub>2</sub> uniformly increases because WSe<sub>2</sub> is doped by electron transfer to WO<sub>x</sub>. Because the amount of transferred electron increases with increasing MoS<sub>2</sub> thickness,  $E_F$  of WSe<sub>2</sub> also changes by MoS<sub>2</sub> thickness and band alignment become type II for 4 and 5L-MoS<sub>2</sub> devices, which is shown by dotted blue line in Fig. 5. The band alignment change due to this charge transfer can be seen as (I) in Fig. 4(b). In this consideration, type III should be obtained for 1L and 2L. However, when MoS<sub>2</sub> thickness is become thin like 1L and 2L, WSe<sub>2</sub> is also expected to be modulated by the top gate. Therefore, by applying  $V_{\text{TG}}$ ,  $E_F$  in WSe<sub>2</sub> as well as MoS<sub>2</sub> is modulated at the same time, resulting to the type II from type III by decreasing MoS<sub>2</sub> thickness, as shown by a dotted orange line in Fig. 5 and (II) in Fig. 4(b). Because of these two different origins for  $p$ -doping reduction in WSe<sub>2</sub>, only 3L MoS<sub>2</sub> shows type III.

Through this study, it is revealed that band alignment of  $p^+$ -WSe<sub>2</sub>/MoS<sub>2</sub> TFET is controlled by the two different physical origins, that is,  $E_F$  modulation in WSe<sub>2</sub> by  $V_{\text{TG}}$  and electron transfer from MoS<sub>2</sub>. Since both origins depends on the MoS<sub>2</sub> channel thickness, the band alignment is quite sensitive to the MoS<sub>2</sub> thickness. This kind of drastic change with MoS<sub>2</sub> thickness happens because  $p$ -doping from WO<sub>x</sub> is not high enough.

**Acknowledgement:** This research was partly supported by The Canon Foundation, the JSAP Core-to-Core Program, A. Advanced Research Networks, JSAP KAKENHI Grant Number JP19H00755, Japan.

**References:** [1] A. M. Ionescu *et al.*, Nature 2011, **479**, 329. [2] J. He *et al.*, Adv. Electron. Mater. 2018, **4**, 1800207.

## Figures

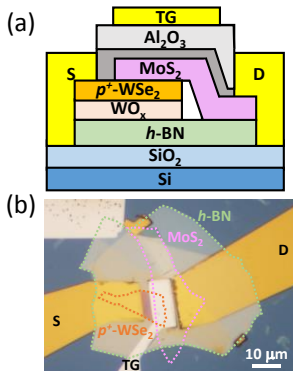


**Figure 1:** (a) Schematic illustration and (b) optical image of the  $p^+$ -WSe<sub>2</sub>/2L-MoS<sub>2</sub> TFET device.

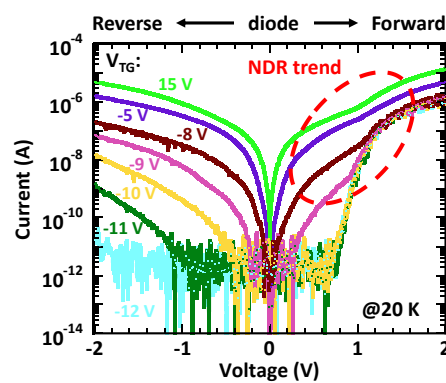


**Figure 2:** Diode properties of  $p^+$ -WSe<sub>2</sub>/3L-MoS<sub>2</sub> TFET at 20 K

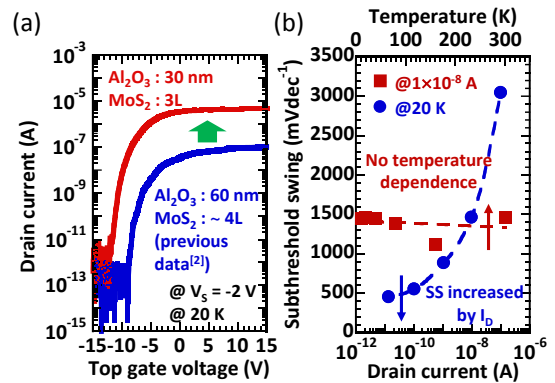


**Figure 3:** (a)  $I_{\text{DS}}-V_{\text{TG}}$  curves of 3L- and 4L-MoS<sub>2</sub> devices. (b) S.S. as functions of  $I_{\text{DS}}$

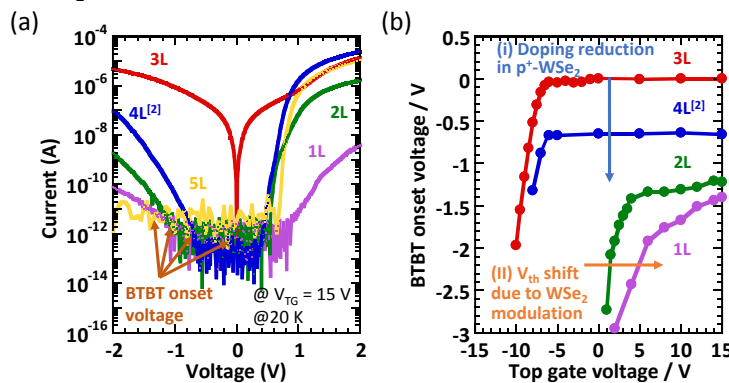


**Figure 4:** (a) Diode properties and (b) BTBT onset voltage as functions of  $V_{\text{TG}}$  for  $p^+$ -WSe<sub>2</sub>/1 - 5L MoS<sub>2</sub> devices.

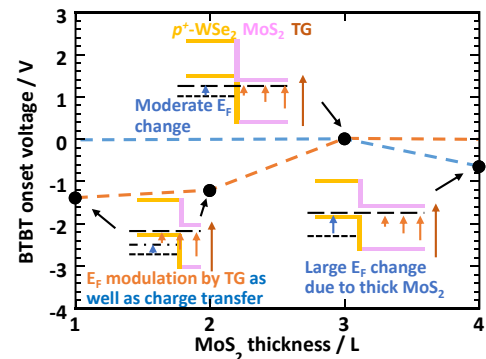


**Figure 5:**  $V_{\text{BTBT}}$  as a function of MoS<sub>2</sub> thickness with the illustration of band alignment at  $V_{\text{TG}} = 15$  V.